Title	Sal-like 4 (SALL4) suppresses CDH1 expression and maintains cell dispersion in basal-like breast cancer.
Author(s)	Itou, Junji; Matsumoto, Yoshiaki; Yoshikawa, Kiyotsugu; Toi, Masakazu
Citation	FEBS letters (2013), 587(18): 3115-3121
Issue Date	2013-09-17
URL	http://hdl.handle.net/2433/191231
Right	© 2013 Federation of European Biochemical Societies. Published by Elsevier B.V.; This is an open access article.
Type	Journal Article
Textversion	publisher

FEBS Letters

CrossMark

Sal-like 4 (SALL4) suppresses CDH1 expression and maintains cell dispersion in basal-like breast cancer

Junji Itou [a],[*],[1], Yoshiaki Matsumoto [a],[b],[1], Kiyotsugu Yoshikawa [a], Masakazu Toi [a],[b]

[a] Laboratory for Malignancy Control Research, Medical Innovation Center, Graduate School of Medicine, Kyoto University, 53 Shogoin-Kawahara-cho, Sakyo-ku, Kyoto 606-8507, Japan
[b] Department of Breast Surgery, Graduate School of Medicine, Kyoto University, 54 Shogoin-Kawahara-cho, Sakyo-ku, Kyoto 606-8507, Japan

ARTICLE INFO

ABSTRACT

In cell cultures, the dispersed phenotype is indicative of the migratory ability. Here we characterized Sal-like 4 (SALL4) as a dispersion factor in basal-like breast cancer. Our shRNA-mediated SALL4 knockdown system and SALL4 overexpression system revealed that SALL4 suppresses the expression of adhesion gene CDH1, and positively regulates the CDH1 suppressor ZEB1. Cell behavior analyses showed that SALL4 suppresses intercellular adhesion and maintains cell motility after cell–cell interaction and cell division, which results in the dispersed phenotype. Our findings indicate that SALL4 functions to suppress CDH1 expression and to maintain cell dispersion in basal-like breast cancer.

© 2013 Federation of European Biochemical Societies. Published by Elsevier B.V. All rights reserved.

1. Introduction

Cell migration is recognized in various fields, including cancer. A hallmark of migratory cells is the dispersed phenotype in in vitro condition, in which a cell located at the edge of a cluster loses intercellular adhesion, possesses membrane spikes and front–rear polarity, and moves away independently from the cluster. In contrast, plated non-migratory cells form compacted clusters, where adhesiveness is augmented, and single dispersed cell is not seen. One of the phenomena to induce the migratory ability is epithelial mesenchymal transition (EMT), by which epithelial properties, e.g., the compacted morphology and epithelial marker expression, are replaced by the dispersed phenotype and mesenchymal gene expression [1]. An advantageous model to study cell dispersion and EMT is basal-like breast cancer. Some of basal-like breast cancer cell lines, such as SUM159 and MDA-MB-231, have

the dispersed phenotype and mesenchymal gene expression. These characteristics are convertible to epithelial properties by genetic manipulation, which allows us to digest what factor(s) functions to control cell dispersion and EMT. For instance, the zinc finger- and homeobox containing transcription factor ZEB1 (also known as deltaEF1 and TCF8) acts as an EMT activator. ZEB1 suppresses the transcription of the adhesion gene CDH1, and ZEB1 knockdown enhances cell–cell adhesion [2]. The miR200 family of microRNAs is known as a suppressor of the ZEB family [3]. Introduction of miR200-mediated ZEB1 silencing diminishes the dispersed phenotype and motility in MDA-MB-231 [4]. CDH1 encodes the cell–cell adhesion protein E-cadherin. MDA-MB-231 having ectopic E-cadherin expression exhibits the compacted epithelial morphology and loss of the migratory ability [5]. These revealed that CDH1 suppression by ZEB1 plays a key role in the maintenance of cell dispersion in basal-like breast cancer.

Sal-like 4 (SALL4) is one of the mammalian homologs of the Drosophila region specific homeotic gene spalt (sal), which encodes a multiple zinc finger transcription factor. SALL4 consists of four exons, and the second of which has an internal splicing donor site. SALL4A, one of two SALL4 variants, is translated from the mRNA having the entire exon2, whereas the mRNA for SALL4B has the short form of exon2 [6]. SALL4 has been identified as a causative factor in acute myeloid leukemia [6]. An increase in SALL4

expression has also been reported in breast- [7,8], lung- [9], colo-rectal- [10] and liver cancers [11] as well as germ cell tumors [12,13]. In addition to in cancerous tissues and cancer cell lines, SALL4 expression has been detected in circulating breast cancer cells [14]. In breast cancer cell lines, *SALL4* transcription is positively regulated by STAT3 [7], and SALL4 suppression provides proliferative inhibition [7,8].

In this study, we identified SALL4 as a cell dispersion factor. We demonstrated that basal-like breast cancer cell lines undergo transition to a compacted epithelial state by SALL4 knockdown. In reciprocal experiments, the overexpression of SALL4 provided the dispersed phenotype and a reduction in *CDH1* expression to epithelial cells. The time-course observation revealed that SALL4 prevents cell–cell adhesion, and maintains cell motility in basal-like breast cancer.

2. Materials and methods

2.1. Cell culture

Basal-like breast cancer cell lines, SUM159 and MDA-MB-231, were purchased from Asterand (Detroit, MI, USA) and ATCC (Manassas, VA, USA), respectively. Dr. Robert A. Weinberg kindly gifted the immortalized human mammary epithelial cells (HMLE) to us. Details of the culture conditions were described in the Supplementary data. For the wound healing assay, an 80–90% confluent monolayer culture was scratched by a 10–200 µl tip.

2.2. Knockdown and overexpression experiments

Lenti vectors, pLKO.1 (Addgene #10878) and pLKO-TetOn (Addgene #21915) were used to express short hairpin RNA (shRNA) and miR200 family. The sequences of shRNAs are, "GCGGACUUGAAGA-AGUCGUGC" for shGFP, "UAGCUUGGCUUGUUUCAAGGC" for shSALL4#3, "UUACUGUGGCUUCAUCCUCAC" for shSALL4#5, "UUAUAUUCAGUAGUGGUCUGG" for shBMI1 and "UUUAACCU-CUUGUAUUGUUGC" for shZEB1. The retrovirus system with pMSCV backbone vector (Life Technologies, Carlsbad, CA, USA) was used to introduce gene overexpression.

2.3. Quantification of mRNA level

To evaluate changes in gene transcription, we analyzed the mRNA levels by quantitative reverse transcription-polymerase chain reaction (RT-PCR). Total RNA samples were obtained from cultures with doxycycline (DOX) for 0.5, 1, 2, 4 and 7 days, and without DOX for 7 days. The primers for mRNA quantification are listed in the Supplementary Table. We used the mean cycle threshold (Ct) values of *ACTB* and *EF1A1* as an internal control, respectively, for the experiments in SUM159 and for in MDA-MB-231 and HMLE. The values of relative mRNA level and standard deviations were calculated according to the Applied Biosystems' instruction. For statistical analyses, the deltaCt value, calculated by subtracting the Ct value of internal control from that of target gene, was used.

2.4. Immunoblotting

Cells were cultured for 7 days with or without DOX induction and lysed. Rabbit anti-SALL4 antibody (Abcam, Cambridge, United Kingdom, ab29112, 1:500), goat anti-ZEB1 antibody (Santa Cruz Biotechnology, Santa Cruz, CA, USA, sc-10572, E-20, 1:200), rabbit anti-Cyclin D1 antibody (Cell Signaling Technology, Danvers, MA, USA, #2978, 92G2, 1:1000) and mouse anti-beta actin antibody (Abcam, ab6276, 1:2500) were used.

2.5. Immunostaining

Cells were cultured for 2 days with or without DOX induction and fixed. Rabbit anti-E-cadherin antibody (Sigma–Aldrich, Saint Louis, MO, USA, SAB4503751, 1:100) and goat anti-rabbit IgG antibody conjugated with Alexa Fluor 488 (Life Technologies, A11008, 1:2000) were used respectively for the primary and secondary antibody reactions. DAPI was used for counter staining.

2.6. Luciferase assay

We used luciferase constructs, phosphoglycerate kinase (PGK) promoter-Luc2, PGK-Luc2-miR200 reporter and ZEB1 promoter-Luc2. Each luciferase construct was transfected to SUM159, and a stable cell line was obtained. The stable cells were infected with the EGFP, miR200 family, shGFP or shSALL4 expression systems, and cultured for 7 days. The number of cells was counted, and 1×10^4 cells were used for the assay. The mean value of PGK-Luc2 stable cells infected with the gene or shRNA expression system was used to normalize the values of corresponding infectants in the miR200 reporter and *ZEB1* promoter assay.

2.7. Imaging

Phase contrast, bright field and fluorescent images were obtained by the all-in-one microscope BZ-9000 Generation II with BZ Analyzer software (Keyence, Osaka, Japan). For time-lapse analyses, differential interference contrast images were obtained at every 10 min with an inverted microscope IX81 (Olympus, Tokyo, Japan). A series of time-lapse images was combined to make a movie by Metamorph software (Molecular Devices, Sunnyvale, CA, USA).

2.8. Statistics

Results of cell morphology, mRNA quantification and cell behavior of SALL4 knockdown experiments in SUM159 were statistically analyzed by the one-way ANOVA, because we compared the value of shSALL4-expressing cells to the values of two controls, no-DOX and shGFP. Growth, cell death, sequential gene expression analysis, immunoblotting, luciferase assay, and experiments with shBMI1 and shZEB1 in SUM159 were analyzed by the Student's *t*-test. The Fisher's exact test was used for analyses of frequencies of cell dispersion and adhesion in the time-lapse analyses. Results of experiments in MDA-MB-231 and HMLE were analyzed by the Student's *t*-test. $P < 0.05$ was considered statistically significant. Error bars in all graphs indicate standard deviations.

3. Results and discussion

3.1. Epithelial transition is induced by SALL4 knockdown in basal-like breast cancer

SALL4 involves in cell proliferation in breast cancer cell lines [7,8]. The functions of SALL4, however, remain elusive. To analyze the functions of SALL4 in breast cancer, we established a DOX inducible shRNA expression system with shGFP and shSALL4 constructs in the basal-like breast cancer cell line SUM159. To evaluate effects of our system, we analyzed the cell proliferative ability, a known function of SALL4. In our system, reduced cell number was observed in cells having shSALL4#3 and #5 expression, but not in shGFP expression (Fig. S1A–C). Target sites of shSALL4#3 and #5 were designed at the regions common to the mRNAs of SALL4 variants. Because the shSALL4#5 is more effective than the #3, we mainly used the #5 in this study. Quantitative RT-PCR

and immunoblotting showed significant reductions in SALL4 mRNA and protein levels in DOX-induced cells (Fig. S1D and E). The ratio between the numbers of dead cells and total cells in shSALL4-expressing cells was identical to that in the no-DOX control (Fig. S1F), indicating that the reduced cell number observed by SALL4 knockdown is not due to decreased cell survival. To analyze changes in expression of the proliferation genes, we quantified the mRNA levels. *BMI1*, a polycomb group gene, is positively regulated by SALL4 [15]. BMI1 suppresses expression of the cyclin-dependent kinase inhibitors, such as *p16*, *p18* and *p21* [16]. In our system, shSALL4 reduced the *BMI1* level and increased the *p16* and *p18* levels (Fig. S2A–D). We analyzed other proliferation markers, *MYC*, *CCNE1* and *CCND1*. It has been reported that SALL4 positively regulates *CCND1* in transcription level [11]. We observed a reduction in expression of *CCND1* in shSALL4-expressing cells (Fig. S2E–G). In protein analysis, Cyclin D1, the product of *CCND1*, level was reduced (Fig. S2H). These results indicate that SALL4 regulates cell proliferation in breast cancer, and our inducible shRNA expression system is useful to explore SALL4 functions.

In in vitro conditions, some of basal-like breast cancer cell lines, including SUM159, tend to be dispersed. Surprisingly, almost cells having shSALL4 expression lost membrane spikes, and formed compacted clusters (Fig. 1A–F). In order to examine this difference, we measured the lengths of perimeters and contacting areas of cells located at the edges of the clusters (Fig. S3). Polarized and spine-rich cells typically have a longer perimeter than spineless cells. We compared the lengths of perimeters of shSALL4-expressing cells to that of no-DOX and shGFP controls. Small values observed in shSALL4-expressing cells indicate that the cells became spineless (Fig. 1G). The ratio of the length of contacting area to that of perimeter reflects the degree of compaction. Cells having shSALL4 expression were more compacted than the controls (Fig. 1H).

Since mammary cells possess a potential to shift between compacted epithelial and dispersed mesenchymal states [2,17], the compaction observed in shSALL4-expressing cells was suggestive of a transition to the epithelial state. Thus, we analyzed mRNA levels of the epithelial marker *CDH1* and the mesenchymal markers *VIM* and *CDH2* (Fig. 1I–K). In shSALL4-expressing cells, the *CDH1* level was increased and the *VIM* level was reduced. The *CDH2* level was not significantly changed. We detected immunoreaction of E-cadherin, the product of *CDH1*, in shSALL4-expressing cells (Fig. 1L–O). Our observations, the compacted phenotype (Fig. 1D, F and H) and the up-regulation of epithelial marker *CDH1* (Fig. 1I and O), indicate that SALL4 knockdown induces the epithelial transition. The previous study has demonstrated that ectopic E-cadherin expression induces the compacted phenotype and reduction in the vimentin, the product of *VIM*, level in basal-like breast cancer MDA-MB-231 [5]. SALL4 might regulate cell dispersion and mesenchymal gene expression by suppressing *CDH1* transcription.

3.2. SALL4 regulates the EMT factor ZEB1

We suspected that SALL4 regulates transcription factors involving in EMT, because SALL4 knockdown induces epithelial transition. In order to identify the factor(s), we used quantitative RT-PCR to screen the transcription factors, *SNAI1*, *SNAI2*, *TWIST1*, *TWIST2*, *FOXC1*, *FOXC2*, *TGFB1*, *TCF3*, *GSC*, *GRHL2*, *ZEB1* and *ZEB2* [18–20]. In the result, we found reduction in the *ZEB1* mRNA level in shSALL4-expressing cells (Fig. 2A), while the others were not significantly changed (Fig. 2B and Fig. S4). No detectable amplification was observed in the experiments for *GSC* and *GRHL2*. In addition to change in the *ZEB1* mRNA level, ZEB1 protein level was reduced in shSALL4-expressing cells (Fig. S5).
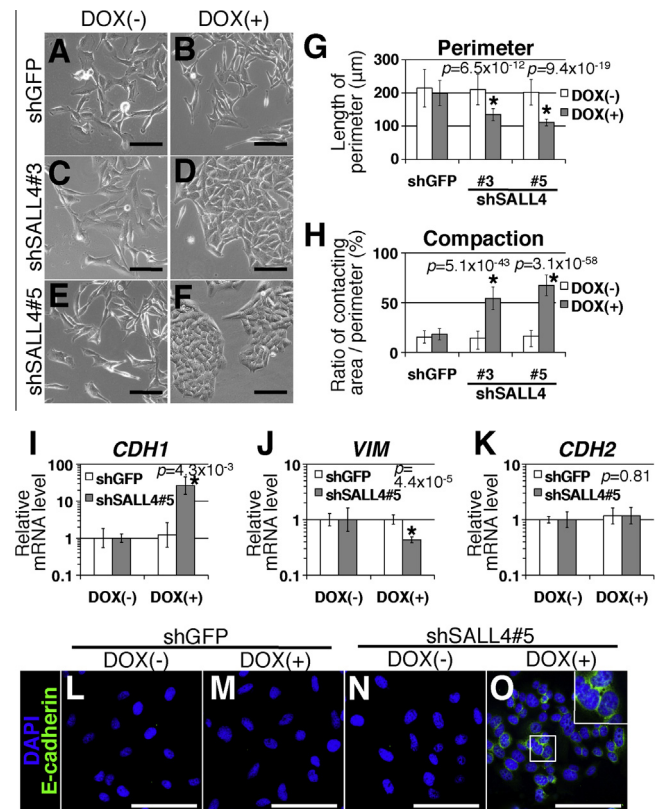

Fig. 1. The compacted phenotype and epithelial gene expression observed by SALL4 knockdown in SUM159. (A–F) Cell compaction was observed in cells having shSALL4 expression. Typical images of cells having inducible shGFP (A and B), shSALL4#3 (C and D) and shSALL4#5 (E and F) are shown. Cells were cultured with (B, D and F) or without DOX (A, C and E) for 7 days. (G and H) The lengths of perimeters and contacting areas were measured in the cells located at the edges of the clusters in the cultures with or without DOX for 7 days. Cells having shSALL4 expression had a shorter perimeter length than control cells (G, n = 30). The ratios of the lengths of contacting area and perimeter were calculated to analyze the degree of compaction. Cells having shSALL4 expression were compacted (H, n = 30). (I–K) mRNA levels were quantified to analyze changes in the expressions of *CDH1* (I, n = 3), *VIM* (J, n = 3) and *CDH2* (K, n = 3) in the cultures with or without DOX for 7 days. (L–O) Immunostaining was performed in shGFP (L and M, n = 3) and shSALL4 (N and O, n = 3). Cells were cultured with (M and O) or without DOX (L and N) for 2 days. Detectable E-cadherin expression (green) was observed in shSALL4-expressing cells. Nuclei were visualized by DAPI (blue). The inset in O is a high magnification image of the boxed area. Scale bars in A–F and L–O indicate 100 μm. Error bars indicate standard deviations. Asterisks indicate statistical significance. (For interpretation of the references to colour in this figure legend, the reader is referred to the web version of this article.)

ZEB1 mRNA is one of known targets of the miR200 family-mediated gene silencing [4,21]. Thus we assessed the activities of miR200s by using a miR200 reporter (Fig. S6), which has the *ZEB1* 3′ untranslated region, a target of miR200 family. To evaluate the miR200 reporter, we introduced expressions of two miR200 regions, miR200b-a-429 and miR200c-141. The expression of miR200 family decreased the luciferase activity (Fig. 2C), indicating that using the miR200 reporter enables us to examine the activities of miR200s-mediated gene silencing. Comparing to the shGFP control, shSALL4-expressing cells showed no alteration of the luciferase activity (Fig. 2D). This result indicates that the activities of miR200s are not changed by SALL4 knockdown. It is known that expressions of the ZEB family and the miR200 family are mutually exclusive [3]. ZEB1 and ZEB2 bind to the promoter regions of miR200 family, and suppress their transcription. The miR200s act as the silencer for *ZEB1* and *ZEB2* mRNAs by binding to their 3′ untranslated regions. A previous study has demonstrated that *ZEB1* knockdown increases miR200s activities [22]. We showed
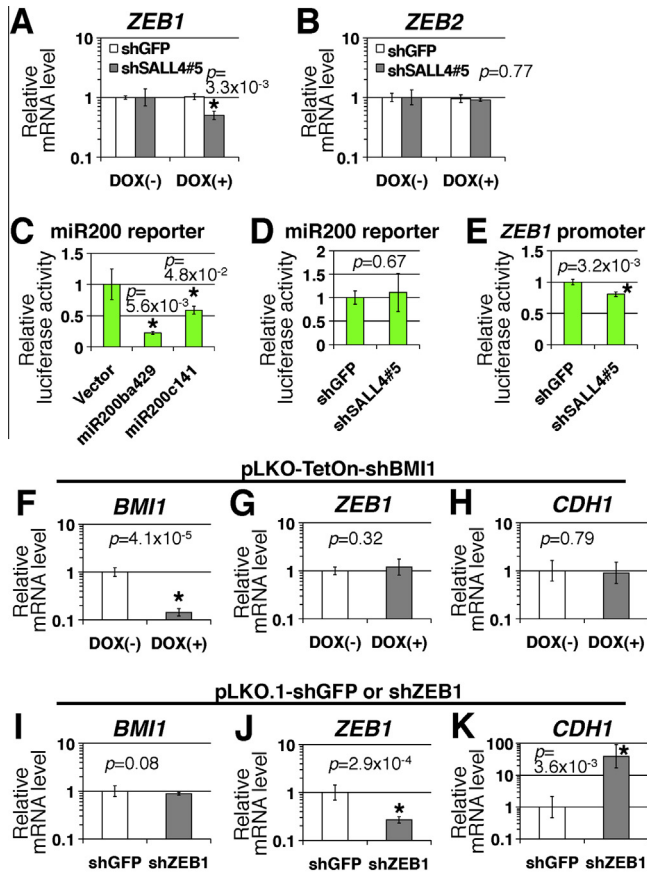
Fig. 2. The SALL4-ZEB1 network in SUM159. (A and B) Quantification of the expression levels of ZEB family transcription factors at 7 days post DOX administration. *ZEB1* expression was reduced by shSALL4 expression (A, n = 3), whereas *ZEB2* was not affected (B, n = 3). (C and D) The activity of the miR200 reporter was reduced by the miR200 family expression (C, n = 3), but not by shSALL4 (D, n = 3). (E) *ZEB1* promoter activity was reduced by shSALL4 expression (n = 3). (F–H) The levels of mRNA were quantified for *BMI1* (F, n = 3), *ZEB1* (G, n = 3) and *CDH1* (H, n = 3) in the cells having DOX inducible shBMI1 expression. (I–K) The levels of mRNA were quantified for *BMI1* (I, n = 3), *ZEB1* (J, n = 3) and *CDH1* (K, n = 3) in the cells having shGFP or shZEB1 expression. Error bars indicate standard deviations. Asterisks indicate statistical significance.

Fig. 3. Sequential gene expression changes after SALL4 knockdown in SUM159. (A–C) Quantification of the mRNA levels for *SALL4* (A, n = 3), *ZEB1* (B, n = 3) and *CDH1* (C, n = 3) were performed at 0.5, 1, 2 and 4 days. The same values of no-DOX controls as for the analyses shown in Fig. S1 (*SALL4*), Fig. 2 (*ZEB1*) and Fig. 1 (*CDH1*) were used to calculate relative values. Error bars indicate standard deviations. Asterisks indicate statistical significance. Data between the no-DOX control and each time point were analyzed by the Student's *t*-test.

reduction in *ZEB1* level (Fig. 2A). However the activities of miR200s were not increased (Fig. 2D). No alteration of miR200s activity observed in shSALL4-expressing cells is likely due to the function of another miR200s suppressor ZEB2, the mRNA level of which was not changed by SALL4 knockdown (Fig. 2B). A similar observation has been reported in a study in ovarian cancer, which showed that the miR200c-141 level was not altered by ZEB1 knockdown in cells expressing ZEB2 [23]. To analyze whether *ZEB1* promoter activity was affected by SALL4 knockdown, we connected the 5 kbp upstream region of the *ZEB1* initiation codon to the luciferase2 gene (Fig. S6). Cells having this *ZEB1* promoter construct showed a reduction in the luciferase activity when shSALL4 was expressed (Fig. 2E), suggesting that SALL4 positively regulates *ZEB1* transcription.

Our results demonstrated that SALL4 regulates two transcriptional regulators, *BMI1* (Fig. S2A) and *ZEB1* (Fig. 2A). To analyze whether BMI1 regulates *ZEB1* transcription, we performed shRNA-mediated *BMI1* knockdown assays. Due to severe proliferative inhibition of *BMI1* knockdown [16], we could not obtain enough number of shBMI1 infectants to analyze the gene expression. We therefore established the DOX inducible shBMI1 expression system to obtain a sufficient number of cells with avoiding the proliferative inhibition. The *ZEB1* mRNA level was not changed by shBMI1
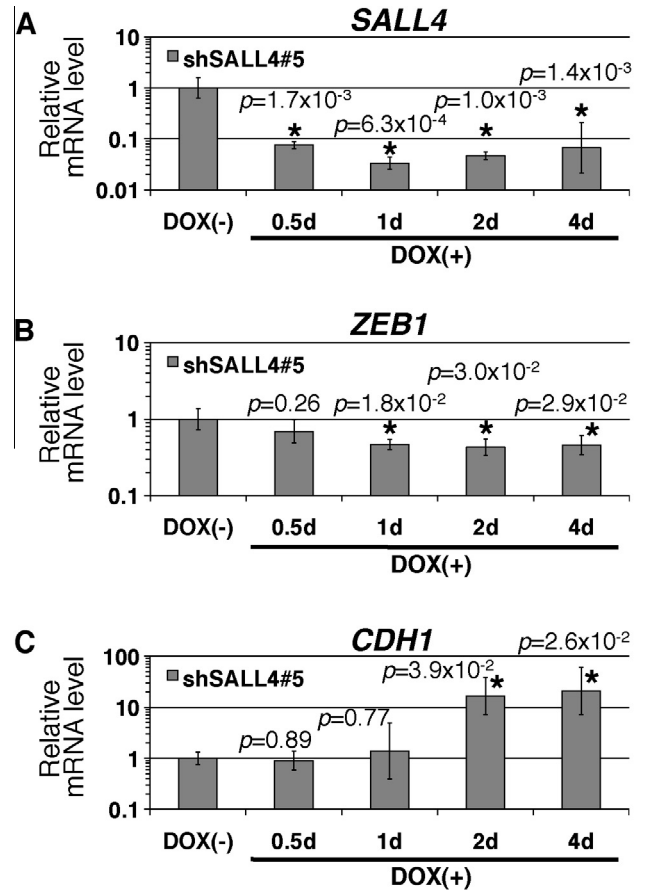
induction (Fig. 2F and G). In head and neck squamous cell carcinoma, *CDH1* transcription is suppressed by BMI1, and BMI1 knockdown increases the E-cadherin level [24]. In basal-like breast cancer, however, the *CDH1* mRNA level was not affected by shBMI1 expression (Fig. 2H). This suggests that the mechanism of *CDH1* regulation is different among cell types.

Besides analyses in shBMI1 expressing cells, we performed ZEB1 knockdown experiments. The *BMI1* mRNA level was not affected by ZEB1 knockdown (Fig. 2I and J). The results of ZEB1 and BMI1 knockdown experiments suggest that these transcriptional regulators are independently regulated by SALL4. Since ZEB1 acts as the suppressor for *CDH1* transcription [2], the *CDH1* mRNA level was up-regulated by shZEB1 expression (Fig. 2K). This suggests that the SALL4-ZEB1 network regulates *CDH1* transcription.

If *CDH1* transcription is suppressed by the SALL4-ZEB1 network, a change in *CDH1* level should be observed after a reduction in *ZEB1* expression when shSALL4 is induced. To analyze the timing of changes in *SALL4*, *ZEB1* and *CDH1* expressions, we performed quantitative RT-PCR in the DOX inducible shSALL4 expression system at time points 0.5, 1, 2 and 4 days post DOX administration. A reduction in the *SALL4* mRNA level was observed from 0.5 day (Fig. 3A). The *ZEB1* level was significantly changed from 1 day (Fig. 3B). An increase in the *CDH1* level was observed from 2 days, suggesting that up-regulation of *CDH1* transcription occurs between 1 and 2 days (Fig. 3C). These results support the suggestion that *CDH1* is suppressed by the SALL4-ZEB1 network in basal-like breast cancer.

3.3. SALL4 maintains cell dispersion and regulates gene expression in MDA-MB-231 as well as in SUM159

The previous study has reported that SALL4 knockdown impairs the proliferative ability in another basal-like breast cancer cell line MDA-MB-231 [7]. To assess the generality of our observation in SUM159, we analyzed the changes in the phenotype and gene expression in MDA-MB-231. Cells having shSALL4 expression lost spikes and exhibited an oval-shape (Fig. 4A and B). However, unlike SUM159, the cells were enlarged. The mean perimeter length of enlarged oval-shaped cells was comparable to that of spine-rich controls (Fig. 4C). SALL4 knockdown increased the degree of compaction in MDA-MB-231 (Fig. 4D). In quantitative RT-PCR analyses for the epithelial and mesenchymal genes, CDH1 expression was augmented, and VIM was reduced (Fig. 4E and F). The CDH2 level was not significantly changed (Fig. 4G). The levels of transcriptional regulators BMI1 and ZEB1 were reduced by SALL4 knockdown (Fig. 4H and Fig. S7). These results, except for the effect on cell size, were similar to the observations in SUM159, suggesting that SALL4 maintains cell dispersion and regulates the expressions of epithelial and mesenchymal genes in basal-like breast cancer cell lines.

3.4. Mammary epithelial cells exhibit the dispersed phenotype and express the mesenchymal genes by SALL4 overexpression

HMLE is utilized as an epithelial cell model in breast cancer studies [17]. We overexpressed SALL4 variants, SALL4A and SALL4B, in HMLE to analyze whether SALL4 induces cell dispersion in compacted epithelial cells. The EGFP control showed compacted clusters (Fig. 5A). The clusters of SALL4A and SALL4B overexpressing cells had more spaces than that of EGFP control (Fig. 5B and C arrowheads). These spaces were likely to be caused by a loss of adhesiveness. In SALL4 overexpressions, cells exhibited membrane spikes, and the mean lengths of perimeters were increased (Fig. 5D). The degrees of compaction were reduced (Fig. 5E). These results imply that SALL4 forces cell dispersion in HMLE. However, SALL4 itself is insufficient to induce complete cell dispersion as in basal-like breast cancers, suggesting that other supportive factor(s) is required to induce it.

In basal-like breast cancers, SALL4 knockdown increases the expression of adhesion gene CDH1 and reduces the levels of mesenchymal genes VIM and ZEB1 (Figs. 1, 2 and 4). We analyzed the mRNA levels of CDH1, VIM and ZEB1 in HMLE having SALL4 overexpression. SALL4A and SALL4B reduced the CDH1 level (Fig. 5F), which might involve in a loss of cell–cell adhesion. Conversely, the VIM and ZEB1 expressions were up-regulated (Fig. 5G and H).
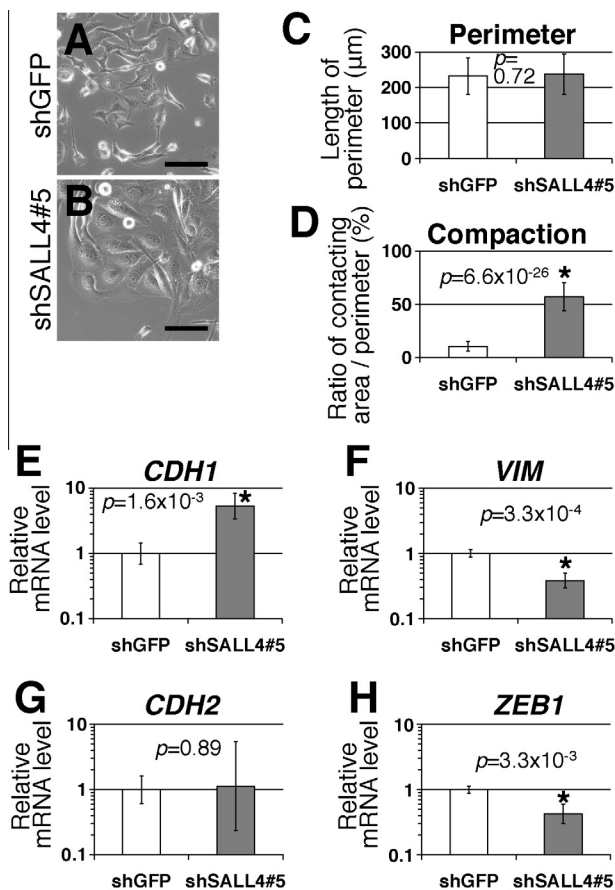

Fig. 4. The compacted phenotype and changes in gene expressions observed by SALL4 knockdown in MDA-MB-231. (A and B) Compaction was seen in cells having shSALL4 expression at 7 days post infection. Typical images of cells having shGFP (A) and shSALL4 (B) are shown. Scale bars indicate 100 μm. (C and D) The lengths of perimeters and contacting areas were measured in the cells located at the edges of the clusters. The perimeter lengths were not changed (C, n = 30). Cells having shSALL4 expression were compacted (D, n = 30). (E–H) Total mRNA was obtained at 7 days post infection, and cDNA was synthesized. The levels of mRNA were quantified to analyze changes in expressions of CDH1 (E, n = 3), VIM (F, n = 3), CDH2 (G, n = 3) and ZEB1 (H, n = 3). Error bars indicate standard deviations. Asterisks indicate statistical significance.
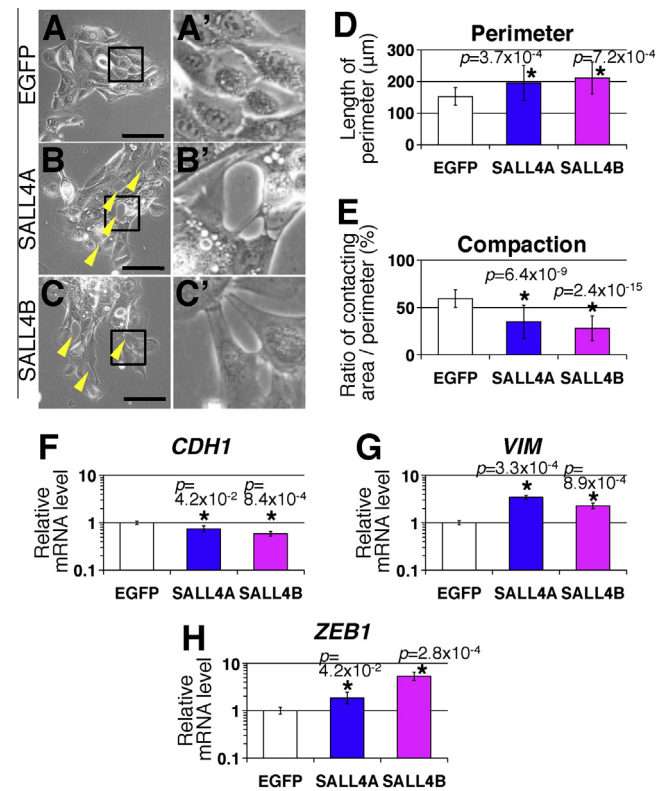

Fig. 5. The dispersed phenotype and mesenchymal gene expression induced by SALL4 overexpression in epithelial cells. (A–C) Typical images of EGFP (A), SALL4A (B) and SALL4B (C) overexpressing epithelial cells. Spaces in clusters were pointed by arrowheads. A′, B′ and C′ are the high magnification images of the boxed areas of A, B and C, respectively. Scale bars indicate 100 μm. (D and E) The lengths of perimeters and contacting areas were measured in the cells located at the edges of the clusters. SALL4 overexpressing cells had a longer perimeter than the EGFP control (D, n = 30). The ratios of the contacting area length to the perimeter length were smaller in cells having SALL4 overexpression than in the EGFP control (E, n = 30). (F–H) The levels of mRNA were quantified to analyze changes in the expressions of CDH1 (F, n = 3), VIM (G, n = 3) and ZEB1 (H, n = 3) by SALL4 overexpression. Error bars indicate standard deviations. Asterisks indicate statistical significance.

Our results suggest that in addition to the maintenance of dispersed phenotype in basal-like breast cancers, SALL4 is capable of inducing cell dispersion with a reduction in CDH1 expression and an increase in the transcription of mesenchymal genes in epithelial cells. Given that SALL4 up-regulates the ZEB1 transcription (Figs. 2A and E, 4H, 5H), and that ZEB1 suppresses the CDH1 transcription (Fig. 2K) [2], the down-regulation of CDH1 was likely to be caused by an ectopic activation of SALL4-ZEB1 network. Since loss of CDH1 function diminishes intercellular adhesiveness in HMLE [25], CDH1 suppression by the SALL4-ZEB1 network might result in a loss of adhesiveness. We observed identical effects between the SALL4A and SALL4B overexpressions in HMLE, indicating that the regulation of cell dispersion is a fundamental function of SALL4.

3.5. SALL4 suppresses cell–cell adhesion to maintain cell dispersion in basal-like breast cancer

Cells having shSALL4 expression exhibited compacted clusters (Fig. 1D and F), suggesting that SALL4 knockdown changes cell behavior. Time-lapse microscopy is utilized to explore cell movements. We performed the time-lapse analyses from 1 to 2 days after starting incubation with DOX in which compaction is initiated in our SALL4 knockdown system. The up-regulation of CDH1 transcription is also initiated between 1 and 2 days post DOX administration (Fig. 3C). The no-DOX controls repeated contact and dispersion (Movie S1). For instance, as shown in Fig. 6A top, one cell interacted with another cell at time point 20 min, and the contact was preserved until 120 min. At 140 min, the cells were uncoupled. Subsequently, one uncoupled cell collided with the other cell at 160 min, and dispersed immediately. In comparison to the control, the contacting period of the cell having shSALL4 expression was extended (Fig. 6A bottom, Movie S2). Cells were interacted at 20 min, and adhered. This contact was persisted for longer than 200 min.

For further understanding of the behavior, we compared the frequencies of cells immediately dispersed, dispersed in 1, 3 and 5 h, and adhered longer than 5 h after cell–cell interaction (Fig. 6B). Most of the control cells were dispersed within 5 h after interaction (78.11%). In shSALL4-expressing cells, the frequencies of dispersion within 5 h were decreased (48.12%), and the rate of formation of intercellular adhesion was increased (21.89–51.88%). In addition, we analyzed the frequencies after cell division (Fig. 6C). Similarly to the results of after cell–cell interaction, the frequencies of dispersion within 5 h were reduced (24.57–5.31%). These suggest that SALL4 knockdown impairs the dispersion ability by enhancing intercellular adhesiveness.

We asked whether shSALL4-expressing cells do not disperse from highly compacted clusters, and whether the compacted clusters move around. We performed the wound healing assay in 80–90% confluent cultures with the proliferation inhibitor mitomycin C (Fig. 7). Because the proliferative ability is different between the control and shSALL4-expressing cells (Fig. S1), inhibition of proliferation was demanded to count the exact number of cells moved into the scratched areas, and to analyze the dispersion ability in the wound healing assay. To determine the concentration of mitomycin C, we performed a growth assay, and found that 0.5 μg/ml of it sufficiently inhibited cell proliferation (Fig. S8). In controls, cells were dispersed and filled the scratched areas (Fig. 7E–G). However the number of cells in the scratched areas was significantly reduced in shSALL4-expressing cells (Fig. 7H and I), indicating that shSALL4-expressing cells do not disperse from their cluster, and that the compacted cluster is immobile. We, moreover, analyzed the speeds of movement in the time-lapse movies used for the analyses shown in Fig. 6. The mean and maximum speeds were not changed between single cells with and without shSALL4 expression (Fig. 8A and B, single). We also analyzed the motility of cells in contact with other cell(s). Although the no-DOX control had an
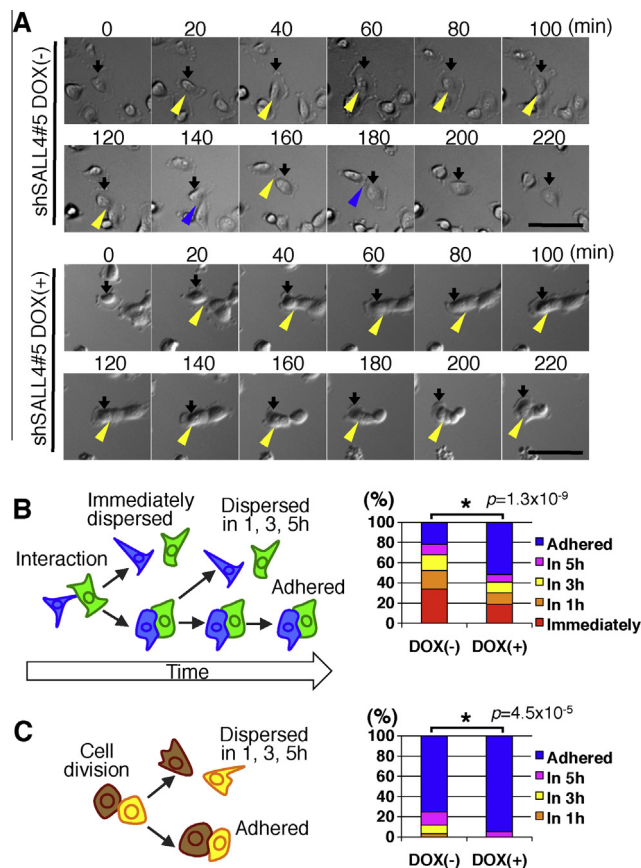

Fig. 6. Attenuation of the dispersion ability in shSALL4-expressing SUM159. (A) Serial pictures of time-lapse microscopy of control (top) and shSALL4-expressing cells (bottom) are shown. Yellow and blue arrowheads point to the contacting state and dispersion, respectively. Arrows indicate the traced cells. Scale bars indicate 100 μm. (B and C) The numbers of occurrences of cell dispersion and adhesion were counted after cell–cell interaction (B, $n = 233$ interactions in DOX($-$), $n = 239$ interactions in DOX($+$)) and cell division (C, $n = 118$ divisions in DOX($-$), $n = 113$ divisions in DOX($+$)). Asterisks indicate statistical significance.
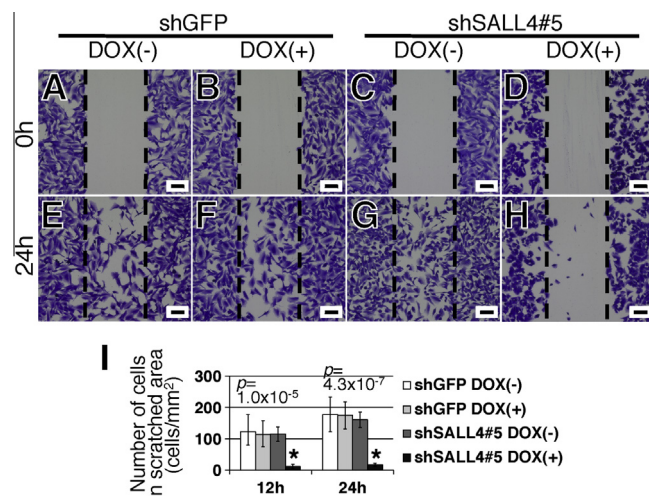

Fig. 7. Loss of migratory ability in compacted shSALL4-expressing SUM159. (A–H) The wound healing assay was performed in shGFP (A, B, E and F)) and shSALL4 (C, D, G and H). Cells were cultured with (B, D, F and H) or without DOX (A, C, E and G) for 7 days. Scratched cultures were stained by crystal violet, and typical images are shown. Dashed lines are depicted to indicate scratched areas. Scale bars indicate 100 μm. (I) The number of cells located in the scratched areas was counted at 12 and 24 h ($n = 6$ positions). Error bars indicate standard deviations. Asterisks indicate statistical significance.
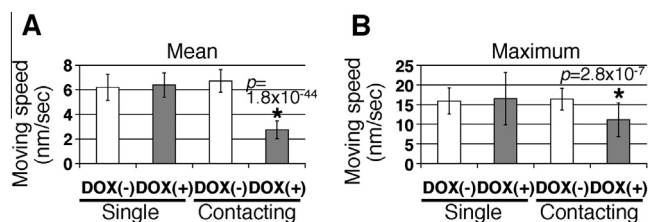
Fig. 8. Attenuation of the motility in contacting shSALL4-expressing SUM159. (A and B) The mean (A) and maximum moving speeds (B) are presented. The moving speed was analyzed in single cell with ($n = 35$) or without DOX ($n = 32$), and in contacting cell with ($n = 40$) or without DOX ($n = 36$). Error bars indicate standard deviations. Asterisks indicate statistical significance.

identical moving speed to single cells, shSALL4-expressing cells showed reduced moving speeds (Fig. 8A and B contacting). The attenuation of the motility observed in contacting shSALL4-expressing cells is consistent with the results of the wound healing assay, and suggests that the trigger to lose cell motility is intercellular adhesion.

We showed that the ability of cell–cell adhesion after interaction and cell division was enhanced in shSALL4-expressing cells (Fig. 6A–C). In epithelial cells, the adhesion protein E-cadherin localizes in the contacting area to form cell–cell adhesion after interaction [26]. Our immunostaining for E-cadherin showed strong signals in the contacting areas (Fig. 1O), supporting the notion that cell–cell adhesion is enhanced by SALL4 knockdown. As exemplified by the wound healing assay and the analysis of moving speeds (Figs. 7 and 8), intercellular adhesion observed in shSALL4-expressing cells persists for more than 24 h, and adhered cells loses their motility. Accumulation of the low-motile adhered cells could develop to compacted clusters. Taken together, SALL4 functions to suppress the formation of cell–cell adhesion to preserve cell motility when cells interact, which contributes to the dispersed phenotype.

In this study, we identified SALL4 as the cell dispersion factor. SALL4 suppresses the adhesion gene *CDH1*, and positively regulates the *CDH1* suppressor *ZEB1*. Consistent with the previous study [5], basal-like breast cancer having shSALL4-induced *CDH1* expression lost the dispersed phenotype. The STAT3 inhibitor impairs the dispersion ability in glioma cells [27]. Given that STAT3 is a positive regulator for *SALL4* transcription in breast cancer [7], our findings are in agreement with the report in glioma cells. Dispersion from an adhesive cluster is one of the characteristics of metastatic cancer [28]. Some of compacted cancer cells acquire the motility and migrate from a cluster to a distant site. Similar events are known in other research fields, such as migratory neural crest cells in development [29] and cardiomyocyte migration in regeneration [30]. Therefore, this study might not only contribute to therapies for cancer metastasis, but also facilitate understanding of the nature of cell migration.

Acknowledgements

Appendix A. Supplementary data

Supplementary data associated with this article can be found, in the online version, at http://dx.doi.org/10.1016/j.febslet.2013.07.049.

References

[1] Kalluri, R. and Weinberg, R.A. (2009) The basics of epithelial–mesenchymal transition. J. Clin. Invest. 119, 1420–1428.

[2] Eger, A. et al. (2005) DeltaEF1 is a transcriptional repressor of E-cadherin and regulates epithelial plasticity in breast cancer cells. Oncogene 24, 2375–2385.

[3] Brabletz, S. and Brabletz, T. (2010) The ZEB/miR-200 feedback loop – a motor of cellular plasticity in development and cancer? EMBO Rep. 11, 670–677.

[4] Park, S.M., Gaur, A.B., Lengyel, E. and Peter, M.E. (2008) The miR-200 family determines the epithelial phenotype of cancer cells by targeting the E-cadherin repressors ZEB1 and ZEB2. Genes Dev. 22, 894–907.

[5] Chao, Y.L., Shepard, C.R. and Wells, A. (2010) Breast carcinoma cells re-express E-cadherin during mesenchymal to epithelial reverting transition. Mol. Cancer 9, 179.

[6] Ma, Y. et al. (2006) SALL4, a novel oncogene, is constitutively expressed in human acute myeloid leukemia (AML) and induces AML in transgenic mice. Blood 108, 2726–2735.

[7] Bard, J.D., Gelebart, P., Amin, H.M., Young, L.C., Ma, Y. and Lai, R. (2009) Signal transducer and activator of transcription 3 is a transcriptional factor regulating the gene expression of SALL4. FASEB J. 23, 1405–1414.

[8] Kobayashi, D., Kuribayshi, K., Tanaka, M. and Watanabe, N. (2011) SALL4 is essential for cancer cell proliferation and is overexpressed in early clinical stages in breast cancer. Int. J. Oncol. 38, 933–939.

[9] Kobayashi, D., Kuribayashi, K., Tanaka, M. and Watanabe, N. (2011) Overexpression of SALL4 in lung cancer and its importance in cell proliferation. Oncol. Rep. 26, 965–970.

[10] Forghanifard, M.M., Moghbeli, M., Raeisossadati, R., Tavassoli, A., Mallak, A.J., Boroumand-Noughabi, S. and Abbaszadegan, M.R. (2013) Role of SALL4 in the progression and metastasis of colorectal cancer. J. Biomed. Sci. 20, 6.

[11] Oikawa, T. et al. (2013) Sal-like protein 4 (SALL4), a stem cell biomarker in liver cancers. Hepatology 57, 1469–1483.

[12] Cao, D., Li, J., Guo, C.C., Allan, R.W. and Humphrey, P.A. (2009) SALL4 is a novel diagnostic marker for testicular germ cell tumors. Am. J. Surg. Pathol. 33, 1065–1077.

[13] Bai, S., Wei, S., Ziober, A., Yao, Y. and Bing, Z. (2013) SALL4 and SF-1 are sensitive and specific markers for distinguishing granulosa cell tumors from yolk sac tumors. Int. J. Surg. Pathol. 21, 121–125.

[14] Panis, C., Pizzatti, L., Herrera, A.C., Cecchini, R. and Abdelhay, E. (2013) Putative circulating markers of the early and advanced stages of breast cancer identified by high-resolution label-free proteomics. Cancer Lett. 330, 57–66.

[15] Yang, J., Chai, L., Liu, F., Fink, L.M., Lin, P., Silberstein, L.E., Amin, H.M., Ward, D.C. and Ma, Y. (2007) Bmi-1 is a target gene for SALL4 in hematopoietic and leukemic cells. Proc. Natl. Acad. Sci. USA 104, 10494–10499.

[16] Siddique, H.R. and Saleem, M. (2012) Role of BMI1, a stem cell factor, in cancer recurrence and chemoresistance: preclinical and clinical evidences. Stem Cells 30, 372–378.

[17] Mani, S.A. et al. (2008) The epithelial–mesenchymal transition generates cells with properties of stem cells. Cell 133, 704–715.

[18] Peinado, H., Olmeda, D. and Cano, A. (2007) Snail, Zeb and bHLH factors in tumour progression: an alliance against the epithelial phenotype? Nat. Rev. Cancer 7, 415–428.

[19] Cieply, B., Pt, Riley, Pifer, P.M., Widmeyer, J., Addison, J.B., Ivanov, A.V., Denvir, J. and Frisch, S.M. (2012) Suppression of the epithelial–mesenchymal transition by Grainyhead-like-2. Cancer Res. 72, 2440–2453.

[20] Xiang, X. et al. (2012) Grhl2 determines the epithelial phenotype of breast cancers and promotes tumor progression. PLoS ONE 7, e50781.

[21] Gregory, P.A., Bert, A.G., Paterson, E.L., Barry, S.C., Tsykin, A., Farshid, G., Vadas, M.A., Khew-Goodall, Y. and Goodall, G.J. (2008) The miR-200 family and miR-205 regulate epithelial to mesenchymal transition by targeting ZEB1 and SIP1. Nat. Cell Biol. 10, 593–601.

[22] Wellner, U. et al. (2009) The EMT-activator ZEB1 promotes tumorigenicity by repressing stemness-inhibiting microRNAs. Nat. Cell Biol. 11, 1487–1495.

[23] Bendoraite, A. et al. (2010) Regulation of miR-200 family microRNAs and ZEB transcription factors in ovarian cancer: evidence supporting a mesothelial-to-epithelial transition. Gynecol. Oncol. 116, 117–125.

[24] Yang, M.H. et al. (2010) Bmi1 is essential in Twist1-induced epithelial–mesenchymal transition. Nat. Cell Biol. 12, 982–992.

[25] Onder, T.T., Gupta, P.B., Mani, S.A., Yang, J., Lander, E.S. and Weinberg, R.A. (2008) Loss of E-cadherin promotes metastasis via multiple downstream transcriptional pathways. Cancer Res. 68, 3645–3654.

[26] Adams, C.L., Chen, Y.T., Smith, S.J. and Nelson, W.J. (1998) Mechanisms of epithelial cell–cell adhesion and cell compaction revealed by high-resolution tracking of E-cadherin-green fluorescent protein. J. Cell Biol. 142, 1105–1119.

[27] Agudelo-Garcia, P.A. et al. (2011) Glioma cell migration on three-dimensional nanofiber scaffolds is regulated by substrate topography and abolished by inhibition of STAT3 signaling. Neoplasia 13, 831–840.

[28] van Zijl, F., Krupitza, G. and Mikulits, W. (2011) Initial steps of metastasis: cell invasion and endothelial transmigration. Mutat. Res. 728, 23–34.

[29] Carmona-Fontaine, C., Matthews, H.K., Kuriyama, S., Moreno, M., Dunn, G.A., Parsons, M., Stern, C.D. and Mayor, R. (2008) Contact inhibition of locomotion in vivo controls neural crest directional migration. Nature 456, 957–961.

[30] Itou, J., Oishi, I., Kawakami, H., Glass, T.J., Richter, J., Johnson, A., Lund, T.C. and Kawakami, Y. (2012) Migration of cardiomyocytes is essential for heart regeneration in zebrafish. Development 139, 4133–4142.